Limitations of two-level emitters as non-linearities in two-photon controlled phase gates

Anders Nysteen,[1] Dara P. S. McCutcheon,[2,1] Mikkel Heuck,[3] Jesper Mørk,[1] and Dirk R. Englund[3]

[1] *DTU Fotonik, Department of Photonics Engineering, Technical University of Denmark, Building 343, 2800 Kgs. Lyngby, Denmark*

[2] *Centre for Quantum Photonics, University of Bristol, Bristol BS8 1TL, United Kingdom*

[3] *Department of Electrical Engineering and Computer Science, Massachusetts Institute of Technology, Cambridge, Massachusetts 02139, USA*

(Dated: December 15, 2016)

We investigate the origin of imperfections in the fidelity of a two-photon controlled-phase gate based on two-level-emitter non-linearities. We focus on a passive system that operates without external modulations to enhance its performance. We demonstrate that the fidelity of the gate is limited by opposing requirements on the input pulse width for one- and two-photon scattering events. For one-photon scattering, the spectral pulse width must be narrow compared to the emitter linewidth, while two-photon scattering processes require the pulse width and emitter linewidth to be comparable. We find that these opposing requirements limit the maximum fidelity of the two-photon controlled-phase gate for Gaussian photon pulses to 84%.

I. INTRODUCTION

A central requirement for quantum computing is a method to coherently interact at least two information carriers. For quantum computing platforms based on photonic qubits, these interactions can be produced by 'off-line non-linearities' consisting of measurements and feed-forward [1–7], or 'in-line' non-linearities based on a non-linear material through which two or more photons interact [8, 9].

Recent experiments have demonstrated major steps towards in-line deterministic controlled phase gates and photonic switches mediated by coupling the polarisation of a single photon to the spin state of an emitter. This has been achieved for Rubidium atoms strongly coupled to optical cavities [10–12], a quantum dot inside a photonic crystal cavity [13], and nitrogen vacancy centers in diamond [14]. Moreover, by applying single-qubit rotations to the atom with $\pi/2$-pulses from external lasers, the atom–cavity systems may function as conditional gates for qubit states encoded in the polarisation of two temporally separated photons [14, 15]. Deterministic switching between two photonic qubits may also be realized by encoding information in other degrees of freedom. Frequency encoding can be used in systems where an emitter is strongly coupled to an optical cavity, where the atom dresses the energy levels of the cavity, resulting in energy levels of the dressed cavity which are not equally spaced [16]. The frequencies of the control and signal photons may be chosen such that the signal only couples to the cavity if the control photon is present [17–19]. The time degree of freedom is used in a scheme proposed by Johne *et al.* [20] and relies on capturing the first of two temporally separated photons. The non-linear interaction in the scheme occurs because of the energy difference of the exciton–bi-exciton transition in a quantum dot placed in an optical cavity, and relies on the ability to detune the dot frequency externally to capture a photon in the quantum dot.

Here we investigate a scheme for a passive controlled-phase gate for two uncorrelated, indistinguishable photons in a dual-rail encoding. The scheme employs two two-level emitters, which mediate photon non-linearities due to their saturability. In contrast to the gates discussed above, the scheme does not rely on any external modulations such as lasers to prepare or alter the emitter states, and it does not require any dynamical trapping processes. Although it has been shown that such a gate can never perform with perfect fidelity [21], the purpose of this work is to understand the limits and origins of its imperfects with a view towards improved future implementations. The considered gate relies on the non-linearity-induced correlations obtained when two photons simultaneously scatter on a non-linear scatterer such as a two-level system [21–24]. We also note, however, that recent developments now allow for the fabrication of very high Q-cavities [25, 26], and if their intrinsic non-linearity dominates the losses, a splitting of the energy spectrum arises through the non-linear Kerr effect [27]. This anharmonic splitting is similar to that in an emitter–cavity system [28], for which the presence of one photon prevents a second photon of the same frequency from coupling to the emitter–cavity system. As such, though we will focus here on using two-level systems such as semiconductor quantum dots, these highly non-linear resonators are also viable candidates as non-linear systems.

This paper is organized as follows. In Section II the basic gate structure and components are introduced, and the gate operation in an idealised case is discussed. In Sections III and IV a more realistic scenario is analysed and the linear and non-linear gate operations are described. A general fidelity measure is considered in Section V to quantify the gate performance, and we conclude our findings in Section VI.

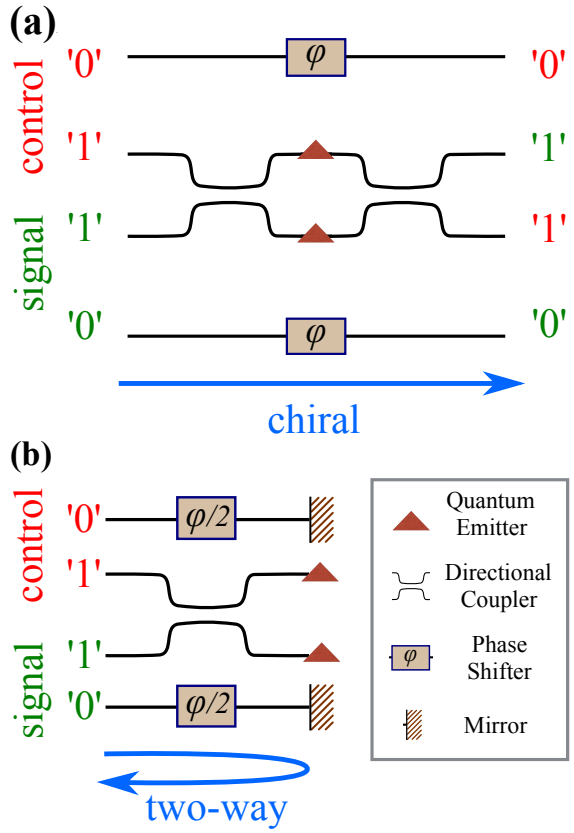

FIG. 1. (a) Schematic of the controlled-phase gate, which uses chiral waveguides, directional couplers, phase shifters, and two identical quantum emitters. The central idea of the gate is that the directional couplers act as 50/50 beam splitters, and as such the input state $|1_c\rangle|1_s\rangle$ gives rise to a Hong–Ou–Mandel bunching effect which can access the inherent non-linearities of the emitters. Only the $|1_c\rangle|1_s\rangle$ input state bunches in this way, while all others transform linearly, thus providing a fundamental non-linear interaction which can realize a two-photon gate. We focus on the chiral setup illustrated in (a), though an equivalent scheme can be realized with convention bi-directional couplers as shown in (b). Note that the '1' arm for the control and signal is interchanged at the output ports in both cases.

II. THE CONTROLLED-PHASE GATE

The structure implementing the gate, shown in Fig. 1, consists of two phase shifters, two directional couplers, and two two-level emitters, which is similar to the systems in Refs. [1, 29, 30]. In Fig. 1(a) we envisage chiral waveguides, for which propagation is permitted only in one direction. We note, however, that an equivalent scheme can be realized by using standard bi-directional waveguides with emitters or perfectly reflecting mirrors placed at their ends, as illustrated in Fig. 1(b). For concreteness we shall focus on the chiral setup of Fig. 1(a), though all of our subsequent analysis equally applies to the two-way setup in Fig. 1(b). The central idea behind the scheme is that the components and waveguides are arranged in such a way that only the combined control and signal input state $|1_c\rangle|1_s\rangle$ accesses the non-linearity of the two-level systems.

To gain some intuition, we first consider quasi-monochromatic input pulses, having a bandwidth much narrower than that of the emitters. Since the state of one photon can affect the state of the other, we must in general consider how pairs of photons are transformed by the gate components. Consider first the evolution of two photons in the state $|0_c\rangle|0_s\rangle$. From Fig. 1 we see that these photons each pick up a phase of φ, producing the transformation $|0_c\rangle|0_s\rangle \to \mathrm{e}^{2\mathrm{i}\varphi}|0_c\rangle|0_s\rangle$. For input states $|1_c\rangle|0_s\rangle$ or $|0_c\rangle|1_s\rangle$, the photon in the $|0\rangle$ state again picks up a phase of φ, while the other passes through the directional couplers and a two-level emitter. The directional couplers act as 50/50 beam splitters, affecting the mode transformation

$$\begin{bmatrix} a_{1c}^\dagger \\ a_{1s}^\dagger \end{bmatrix} \longrightarrow \frac{1}{\sqrt{2}} \begin{bmatrix} 1 & -\mathrm{i} \\ -\mathrm{i} & 1 \end{bmatrix} \begin{bmatrix} a_{1c}^\dagger \\ a_{1s}^\dagger \end{bmatrix}, \tag{1}$$

where $a_{1c}^\dagger|\phi\rangle = |1_c\rangle$ and $a_{1s}^\dagger|\phi\rangle = |1_s\rangle$ with $|\phi\rangle$ denoting the vacuum. In this simplistic monochromatic scenario, let us assume a single photon incident on the emitter acquires a phase of θ. Then the combined effects of the two directional couplers and the emitter cause the transformation $|1_s\rangle \to -i\mathrm{e}^{\mathrm{i}\theta}|1_c\rangle$ and $|1_c\rangle \to -i\mathrm{e}^{\mathrm{i}\theta}|1_s\rangle$. Therefore the photonic states transform as $|1_c\rangle|0_s\rangle \to -i\mathrm{e}^{\mathrm{i}\varphi}\mathrm{e}^{\mathrm{i}\theta}|1_s\rangle|0_s\rangle$ and $|0_c\rangle|1_s\rangle \to -i\mathrm{e}^{\mathrm{i}\varphi}\mathrm{e}^{\mathrm{i}\theta}|0_c\rangle|1_c\rangle$. Considering now the input state $|1_c\rangle|1_s\rangle$, we find that the action of the first directional coupler is to give rise to the Hong–Ou–Mandel interference effect; immediately after the first directional coupler we have a state proportional to $((a_{1c}^\dagger)^2 + (a_{1s}^\dagger)^2)|\phi\rangle$, in which two photons are incident on each emitter in superposition. We denote the phase acquired by a two-photon state passing through an emitter as χ, and therefore find that following the second directional coupler we have the transformation $|1_c\rangle|1_s\rangle \to (-\mathrm{i})^2\mathrm{e}^{\mathrm{i}\chi}|1_c\rangle|1_s\rangle$.

Collecting these results and relabelling $-\mathrm{i}|1_s\rangle \to |1_c\rangle$ and $-\mathrm{i}|1_c\rangle \to |1_s\rangle$ we find

$$\begin{aligned} |0_\mathrm{c}\rangle|0_\mathrm{s}\rangle &\longrightarrow \mathrm{e}^{2\mathrm{i}\varphi}|0_\mathrm{c}\rangle|0_\mathrm{s}\rangle \\ |0_\mathrm{c}\rangle|1_\mathrm{s}\rangle &\longrightarrow \mathrm{e}^{\mathrm{i}\varphi}\mathrm{e}^{\mathrm{i}\theta}|0_\mathrm{c}\rangle|1_\mathrm{s}\rangle \\ |1_\mathrm{c}\rangle|0_\mathrm{s}\rangle &\longrightarrow \mathrm{e}^{\mathrm{i}\varphi}\mathrm{e}^{\mathrm{i}\theta}|1_\mathrm{c}\rangle|0_\mathrm{s}\rangle \\ |1_\mathrm{c}\rangle|1_\mathrm{s}\rangle &\longrightarrow \mathrm{e}^{\mathrm{i}\chi}|1_\mathrm{c}\rangle|1_\mathrm{s}\rangle. \end{aligned} \tag{2}$$

If the emitters acted as linear optical elements, we would have $\chi = 2\theta$. Absorbing the phases φ and θ into the definitions of $|0\rangle$ and $|1\rangle$ respectively, the transformation is locally equivalent to the identity and therefore does not mediate any two-photon interaction. However, if the emitter–photon interaction can be tailored such that $\theta = \varphi$ and $\chi = 2\varphi + \pi$, the transformation in Eq. (2) becomes proportional to the desired control phase gate unitary $\mathrm{diag}(1, 1, 1, -1)$. As such, if the conditions $\theta = \varphi$ and $\chi = 2\varphi + \pi$ can be met a controlled-phase gate is realized. Though we do not expect this to be possible with perfect accuracy [21], in what follows we shall explore the dif-

fering requirements on the pulse shape relative to the emitter linewidth which these conditions impose.

In addition to the two-level-emitters, the other essential components of the gate are the directional couplers needed to produce the transformation in Eq. (1) and induce the Hong–Ou–Mandel effect for the input state $|1_c\rangle|1_s\rangle$. These components may be realized in various waveguide technologies, such as silica-on-silicon ridge waveguides [31], GaAs photonic ridge waveguide circuits [32], photonic crystals waveguides [33], or silicon on insulator platforms [34], where in all cases the length of the coupling region must be engineered such the symmetrical beam splitter relation in Eq. (1) is achieved. We also note, that due to the choice of directional coupler, the output port of the '1' control and signal states are swapped, as indicated in Fig. 1(a). This amounts to nothing more than notation, and could easily be rectified by introducing a crossover between the two '1' outputs.

For proper functionality of the gate, the input states $|0_\mathrm{c}\rangle|0_\mathrm{s}\rangle$, $|1_\mathrm{c}\rangle|0_\mathrm{s}\rangle$, and $|0_\mathrm{c}\rangle|1_\mathrm{s}\rangle$, which only experience linear scattering effects, and the input state $|1_\mathrm{c}\rangle|1_\mathrm{s}\rangle$, which undergoes a non-linear transformation, must all provide the desired output states in Eq. (2) when $\theta = \varphi$ and $\chi = 2\varphi + \pi$. These scattering-induced changes are investigated below, treating the linear and non-linear case separately.

III. LINEAR GATE INTERACTIONS

Let us now consider the gate components in more detail and analyse the conditions under which the scheme can be realized for more realistic non-monochromatic pulsed photon inputs. We describe a single photon pulse in the $|0_c\rangle$ state as

$$|0_c\rangle = \int_{-\infty}^{\infty} \mathrm{d}k\, \xi(k)\, a_{0c}^\dagger(k)|\phi\rangle, \tag{3}$$

where $\xi(k)$ is the spectral profile of the pulse, and $a_{0c}^\dagger(k)$ is the creation operator of photons in the control '0' waveguide with momentum k. Note that we consider a rotating frame such that k is measured relative to the carrier momentum, $k_0 = \omega_0/c$. The simple transformations in Eq. (2) are not generally valid for photonic wavepackets comprised by many k-modes because the phases φ and θ depend on k. In a large-scale system, the output from one gate must function as the input to another gate and they should therefore only differ by a time-translation, which in momentum space corresponds to the transformation $\xi(k) \to \xi(k)\mathrm{e}^{i\varphi(k)}$ with

$$\varphi(k) = \varphi_0 + kL, \tag{4}$$

where L is an additional optical path length of the '0' waveguides, either induced by a change in the refractive index of the material or by a longer arm length.

When $\varphi(k)$ is of the form in Eq. (4), the input state $|0_\mathrm{c}\rangle|0_\mathrm{s}\rangle$ is described by a product of two single-photon states of the form in Eq. (3), and we write the corresponding output state as $|0_\mathrm{c}\rangle|0_\mathrm{s}\rangle \to |\tilde{0}_c\rangle|\tilde{0}_s\rangle$ with

$$|\tilde{0}_c\rangle = -\int_{-\infty}^{\infty} \mathrm{d}k\, \xi(k)\mathrm{e}^{ikL}\, a_{0c}^\dagger(k)|\phi\rangle, \tag{5}$$

and a similar definition for $|\tilde{0}_s\rangle$. Photon pulses with states of this form will be considered our 'ideal' output states, since they are identical to the input state up to a linear frequency-dependent phase corresponding to a fixed temporal delay. The choice of $\varphi_0 = \pi$ has been chosen in anticipation of the transformation of the $|0_\mathrm{c}\rangle|1_\mathrm{s}\rangle$ state discussed below.

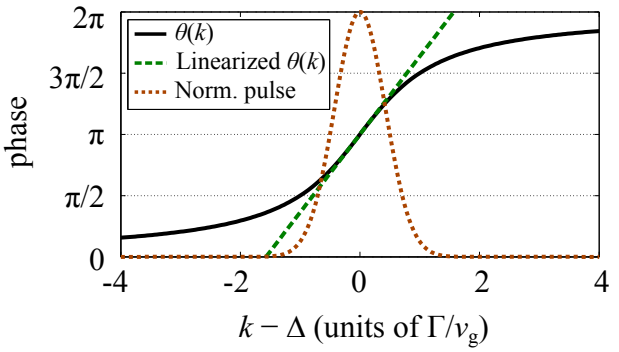

FIG. 2. Phase $\theta(k)$ acquired by a single-photon wavepacket component with moment k propagating in a chiral waveguide scattering on a lossless resonant emitter (black solid line), together with a linear approximation, see Eq. (8) (green dashed line). By comparison, the spectrum of a resonant Gaussian wavepacket with spectral FWHM of $\sigma = \Gamma/(v_\mathrm{g})$ is shown (orange dotted line) with a scaled intensity to match the plotting window.

We now consider changes to the two input states with a single photon in one of the '1' arms, $|0_\mathrm{c}\rangle|1_\mathrm{s}\rangle$ and $|1_\mathrm{c}\rangle|0_\mathrm{s}\rangle$. The photon in the '0' arm is treated analogously to Eq. (5), while that in the '1' arm instead interacts with an emitter. Photons passing through the '1' arms must also give rise to states differing from input states only by a time-translation. To see the conditions under which this is the case, we consider a single-photon pulse as described by Eq. (3) scattering on a two-level emitter in a chiral waveguide. The photon will acquire a complex coefficient $t(k)$ for each momentum component k, resulting in a pulse with spectral profile $t(k)\xi(k)$. The frequency-dependent transmission coefficient is [35, 36],

$$t(k) = \frac{k - \Delta - \mathrm{i}(\Gamma - \gamma)/v_\mathrm{g}}{k - \Delta + \mathrm{i}(\Gamma + \gamma)/v_\mathrm{g}}, \tag{6}$$

where v_g is the group velocity in the waveguide, Δ the momentum detuning of the emitter from the pulse carrier frequency, Γ the emitter decay rate into waveguide modes, and γ the loss rate into modes outside the waveguide [36]. Recalling the effect of the directional couplers, we find that the states transform as $|0_c\rangle|1_s\rangle \to -i|\tilde{0}_c\rangle|\bar{1}_c\rangle$ and $|1_c\rangle|0_s\rangle \to -i|\bar{1}_s\rangle|\tilde{0}_s\rangle$, where

$$|\bar{1}_c\rangle = \int_{-\infty}^{\infty} \mathrm{d}k\, \xi(k)t(k)\, a_{1c}^\dagger(k)|\phi\rangle, \tag{7}$$

with a similar definition for $|\bar{1}_s\rangle$. As previously discussed, we can simply relabel what we refer to as the control and signal photons in the outputs, and absorb factors of $-\mathrm{i}$ in these definitions. We then have $|0_c\rangle|1_s\rangle \rightarrow |\tilde{0}_c\rangle|\bar{1}_s\rangle$ and $|1_c\rangle|0_s\rangle \rightarrow |\bar{1}_c\rangle|\tilde{0}_s\rangle$. What is required, however, is that each photon has a spectral profile identical to an 'ideal' state, $|\tilde{1}_c\rangle$ or $|\tilde{1}_s\rangle$, defined as in Eq. (5) with $a^\dagger_{0c}$ replaced with $a^\dagger_{1c}$ or $a^\dagger_{1s}$.

In the loss-less case, where $\gamma = 0$ and $|t(k)| = 1$, we can write $t(k) = \exp[\mathrm{i}\theta(k)]$. The phase $\theta(k)$ is shown as a function of k in Fig. 2. If the incoming single-photon pulse has a carrier frequency corresponding to the emitter transition frequency, $\Delta = 0$, the phase can be Taylor expanded around $k/\tilde{\Gamma} = 0$, producing

$$\theta(k) = \pi + 2\frac{k}{\tilde{\Gamma}} + \mathcal{O}\left(\frac{k}{\tilde{\Gamma}}\right)^3, \tag{8}$$

where $\tilde{\Gamma} = \Gamma/v_\mathrm{g}$. Keeping the condition $\varphi = \theta$ in mind and comparing Eqs. (4) and (8), we see that a good gate performance requires $|k| \ll \tilde{\Gamma}$, which corresponds to pulses with a spectrum that is much narrower than the emitter linewidth. For spectrally broader pulses for which $\xi(k)$ extends beyond $k \sim \tilde{\Gamma}$, terms of higher order in k will have an influence and introduce chirping effects [23, 24].

To illustrate this in more detail for a specific case, let us consider a Gaussian single-photon wavepacket, defined by the spectral profile

$$\xi(k) = (\pi\sigma'^2)^{-1/4}\exp[-k^2/(2\sigma'^2)], \tag{9}$$

where the spectral bandwidth (FWHM of the intensity spectrum) is $\sigma = 2\sqrt{\ln(2)}\sigma'$. In Fig. 3 we plot the magnitude of the overlap between the desired (ideal) state and actual state for a Gaussian pulse as described above. As expected, the overlap increases when the spectral pulse width, σ, is decreased. The optimum additional path length, L, approaches $L = 2v_\mathrm{g}/\Gamma$ as σ is decreased, which is expected from the linear term in Eq. (8). For larger pulse widths, the optimum L decreases because a straight line with a slope smaller than $2v_\mathrm{g}/\Gamma$ approximates the phase $\theta(k)$ better in this case, as seen in Fig. 2.

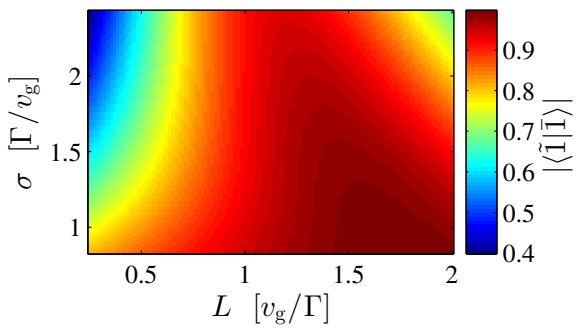

FIG. 3. Overlap between the ideal and scattered state for logical inputs $|1_c\rangle|0_s\rangle$ or $|0_c\rangle|1_s\rangle$ as a function of the additional optical length of the '0' arms, L, and the input pulse width σ defined in Eq. (9).

IV. NON-LINEAR GATE INTERACTIONS

The non-linear interaction occurs for the input state $|1_\mathrm{c}\rangle|1_\mathrm{s}\rangle$, where two photons may be present at the scatterers simultaneously, introducing non-linear interactions through a two-photon bound state [22]. The non-linear scattering is treated by the scattering matrix formalism following Ref. [22], and we include the directional coupler when calculating the scattered state of the entire gate. The gate input consists of two uncorrelated identical photons which we describe by

$$|\psi_\mathrm{in}\rangle = \int_{-\infty}^{\infty}\int_{-\infty}^{\infty}\mathrm{d}k\,\mathrm{d}k'\,\xi(k)\xi(k')a^\dagger_{c1}(k)a^\dagger_{s1}(k')|\phi\rangle. \tag{10}$$

Following the action of the first directional coupler, scattering on the two-level emitters, and passing through the second directional coupler, we find $|\psi_\mathrm{in}\rangle \rightarrow |\psi_\mathrm{scat}\rangle$ with the total scattered state given by

$$|\psi_\mathrm{scat}\rangle = \int_{-\infty}^{\infty}\int_{-\infty}^{\infty}\mathrm{d}k\,\mathrm{d}k'\,\beta_\mathrm{scat}(k,k')a^\dagger_{c1}(k)a^\dagger_{s1}(k')|\phi\rangle, \tag{11}$$

where we have removed a factor of $(-\mathrm{i})^2$ to be consistent with our definitions of the output states, and

$$\beta_\mathrm{scat}(k,k') = \beta^\mathrm{linear}_\mathrm{scat}(k,k') + \frac{1}{2}b(k,k'), \tag{12}$$

with the linear contribution given by $\beta^\mathrm{linear}_\mathrm{scat}(k,k') = t(k)t(k')\xi(k)\xi(k')$ and a non-linear scattering contribution by

$$b(k,k') = \int_{-\infty}^{\infty}dp\;\xi(p)\xi(k+k'-p)B_{kk'p(k+k'-p)}. \tag{13}$$

The scatterer-dependent coefficient $B_{kk'pp'}$ is evaluated in Ref. [36] for a two-level system,

$$B_{kk'pp'} = \mathrm{i}\frac{\sqrt{2\Gamma/v_\mathrm{g}}}{\pi}s(k)s(k')[s(p)+s(p')], \tag{14}$$

where

$$s(k) = \frac{\sqrt{2\Gamma/v_\mathrm{g}}}{k-\Delta+\mathrm{i}(\Gamma+\gamma)/(v_\mathrm{g})}. \tag{15}$$

The ideal output state in the non-linear case is

$$|\tilde{1}_c\rangle|\tilde{1}_s\rangle = -\int_{-\infty}^{\infty}\int_{-\infty}^{\infty}\mathrm{d}k\,\mathrm{d}k'\,\mathrm{e}^{i(k+k')L}a^\dagger_{c1}(k)a^\dagger_{s1}(k')|\phi\rangle, \tag{16}$$

where the minus sign accounts for the required phase flip that defines the controlled-phase gate.

To gain some insight into how well the actual state, $|\psi_\mathrm{scat}\rangle$, approximates the ideal state in Eq. (16), we plot the magnitude of their overlap as a function of L and σ in Fig. 4, again for Gaussian input pulses. In contrast to the one-photon scattering case in Fig. 3, we

now see that the largest overlap is observed for pulse widths $\sigma \approx 2.2\Gamma/v_g$. This is because it is for these widths that the non-linearities are strongest and the required π-phase shift can be generated, consistent with the results in Ref. [23][37]. Furthermore, the optimal value of L in this non-linear scattering case is significantly lower than in the linear case. A comparison of Figs. 3 and 4 demonstrates that limitations in the gate performance are expected to occur because of these different requirements on σ and L to optimally approximate the ideal output states in the linear and non-linear cases, which we now explore in more detail below.

V. FIDELITY OF THE GATE OPERATION

In order to find the optimal pulse width σ and path length difference L, we now consider the operation of the gate as a whole. When incorporated into a larger optical circuit, the logical input state of the gate will necessarily be unknown, and the gate must therefore be able to operate for any linear combination of the four possible logical input states. As such, the gate performance must be quantified by a fidelity based on a worst case scenario, in which the output state of the gate is compared to the ideal target output state, minimised over all possible input states. A gate fidelity meeting these requirements is defined as [38]

$$F(\hat{U},\hat{\mathcal{E}}) \equiv \min_{|\psi\rangle} F_s\big(\hat{U}|\Psi\rangle\langle\Psi|\hat{U}^\dagger, \hat{\mathcal{E}}(|\Psi\rangle\langle\Psi|)\big), \qquad (17)$$

where $\hat{U}$ and $\hat{\mathcal{E}}$ describe the transformations of the ideal and actual gate, respectively, and F_s is the state fidelity defined by [38]

$$F_s(\hat{\rho},\hat{\sigma}) \equiv \mathrm{Tr}\left\{\sqrt{\hat{\rho}^{\frac{1}{2}}\hat{\sigma}\hat{\rho}^{\frac{1}{2}}}\right\}, \qquad (18)$$

for two density operators, $\hat{\rho}$ and $\hat{\sigma}$. The arbitrary input state, $|\Psi\rangle$, is given by

$$\begin{aligned}|\Psi\rangle &= \big(\alpha|0_s\rangle + \beta|1_s\rangle\big)\otimes\big(\zeta|0_c\rangle + \vartheta|1_c\rangle\big)\\ &= \alpha\zeta|00\rangle + \alpha\vartheta|01\rangle + \beta\zeta|10\rangle + \beta\vartheta|11\rangle, \qquad (19)\end{aligned}$$

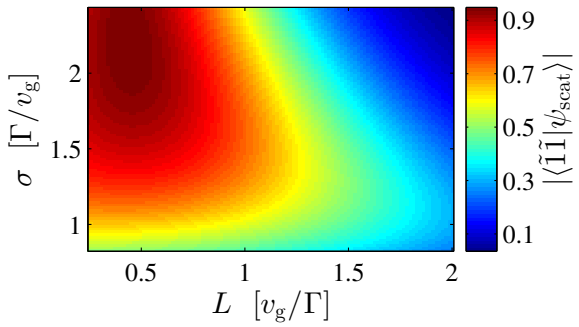

FIG. 4. Overlap between the ideal and scattered state for the $|1_c\rangle|1_s\rangle$ input as a function of the additional optical length of the '0' arms, L, and the input pulse width, σ.

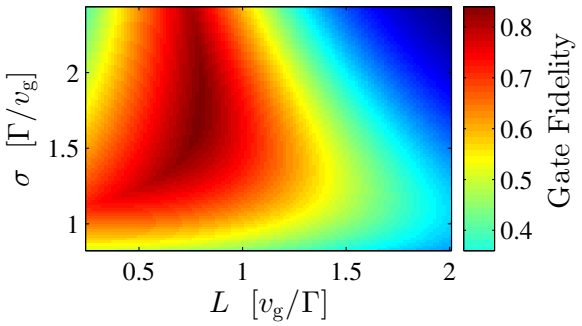

FIG. 5. Gate fidelity as a function of the additional optical length of the '0' arms, L, and the input pulse width, σ.

where $|0_s\rangle|0_c\rangle \equiv |00\rangle$ etc. Using the definitions from previous sections, the ideal gate transformation is

$$\hat{U}|\Psi\rangle = \alpha\zeta|\tilde{0}\tilde{0}\rangle + \alpha\vartheta|\tilde{0}\tilde{1}\rangle + \beta\zeta|\tilde{1}\tilde{0}\rangle - \beta\vartheta|\tilde{1}\tilde{1}\rangle. \qquad (20)$$

If we neglect loss, the output states are pure and the actual (possibly imperfect) transformation is described by $\hat{\mathcal{E}}(|\Psi\rangle\langle\Psi|) = \hat{T}|\Psi\rangle\langle\Psi|\hat{T}^\dagger$, with

$$\hat{T}|\Psi\rangle = \alpha\zeta|\tilde{0}\tilde{0}\rangle + \alpha\vartheta|\tilde{0}\bar{1}\rangle + \beta\zeta|\bar{1}\tilde{0}\rangle + \beta\vartheta|\psi_{\mathrm{scat}}\rangle, \qquad (21)$$

where $|\psi_{\mathrm{scat}}\rangle$ is given by Eq. (11). For pure states, Eq. (18) simplifies to $F_s(|a\rangle\langle a|, |b\rangle\langle b|) = |\langle a|b\rangle|$, and the state fidelity is therefore

$$\begin{aligned}&F_s(\hat{U}|\Psi\rangle\langle\Psi|\hat{U}^\dagger, \hat{T}|\Psi\rangle\langle\Psi|\hat{T}^\dagger) = |\langle\Psi|\hat{U}^\dagger\hat{T}|\Psi\rangle| =\\ &\Big||\alpha\zeta|^2 + \langle\tilde{1}|\bar{1}\rangle\left(|\alpha\vartheta|^2 + |\beta\zeta|^2\right) - |\beta\vartheta|^2\langle\tilde{1}\tilde{1}|\psi_{\mathrm{scat}}\rangle\Big|. \qquad (22)\end{aligned}$$

To find the fidelity of the gate for a given pulse width and path length difference, this state fidelity must be minimised over all possible logical input states $|\Psi\rangle$ parameterised by the coefficients $\alpha, \beta, \zeta, \vartheta$. Since the state fidelity only depends on the magnitude of the coefficients and the signal and control input states both must be normalized, the minimization in Eq. (17) can be carried out by varying only, e.g. $|\alpha|$ and $|\zeta|$. By performing this minimization for different values of σ and L, the trade-offs due to the effects of linear and non-linear scattering can be quantified. The result is shown in Fig. 5, where the gate fidelity is plotted as a function of L and σ, again for Gaussian pulses. The optimum set of parameters is seen to be close to that in Fig. 4 but shifted towards smaller pulse widths and larger L, where the optimum was observed in Fig. 3. This trend is expected, since Eq. (22) effectively performs a weighted average of the overlaps in Figs. 3 and 4. In order to confirm that the gate fidelity corresponds to a worse case scenario, Fig. 6 shows the dependence of the state fidelity on the input states for the optimum parameter set in Fig. 5. It shows that the state fidelity approaches unity for the state $|0_c\rangle|0_s\rangle$, and is above 84% for the entire state space, as expected.

Finally, we note that our formalism easily allows for pulse shapes other than Gaussians to be considered. Most notably, we find that Lorentzian spectral

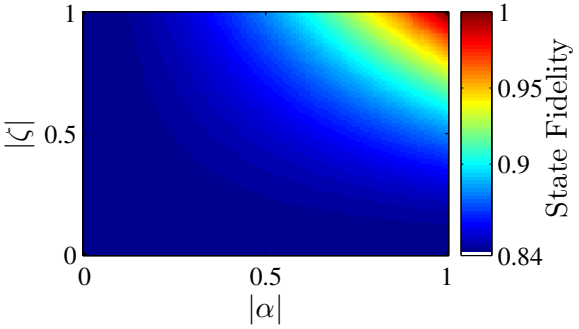

FIG. 6. State fidelity as a function of input states expressed by $|\alpha|$ and $|\zeta|$ for $L = 0.80v_g/\Gamma$ and $\sigma = 1.72\Gamma/v_g$ corresponding to the maximum gate fidelity in Fig. 5.

profiles result in a worse gate fidelity of $F \approx 62\%$. Although a Lorentzian single-photon pulse is expected to most efficiently populate a two-level-emitter, two such coincident pulses give rise to a smaller induced non-linearity [24], which is an essential requirement for the gate to operate. We find that sech^2 pulses achieve a fidelity marginally better than Gaussian pulses, raising the gate fidelity by only 0.5%. Ultimately active modification of pulse shapes may be necessary if gates based on two-level-emitter non-linearities are to attain fidelities approaching unity [29].

VI. CONCLUSION

We have investigated in detail the feasibility of using two-level-emitter non-linearities to construct a passive two-photon controlled phase gate, elucidating the scattering-induced changes to the phase of the pulse and also non-linearity-induced changes in the pulse spectrum. We find that these effects ultimately limit the fidelity of a controlled phase gate based on two-level-emitter non-linearities, giving $F \approx 84\%$ for Gaussian input pulses. The fidelity observed here is, however, comparable to fidelities reported for two-photon gates which instead exploit a dynamical capture of the first photon in a strongly coupled emitter-cavity system [15, 20]. In addition, the dynamical capture necessitates perfect timing of the cavity detuning relative to the arrival time of the pulse, which is avoided in the present case.

ACKNOWLEDGMENTS

AN and JM acknowledge support from NATEC and SIQUTE. DPSM acknowledges support from a Marie Skłodowska Curie Individual Fellowship (ESPCSS). MH acknowledges support from DFF:1325-00144. DE acknowledges support from AFOSR MURI for Optimal Measurements for Scalable Quantum Technologies (FA9550-14-1-0052) and the Air Force Research Laboratory RITA program (FA8750-14-2-0120).

[1] E. Knill, R. Laflamme, and G. J. Milburn, Nature **409**, 46 (2001), ISSN 0028-0836.
[2] P. Kok, W. J. Munro, K. Nemoto, T. C. Ralph, J. P. Dowling, and G. J. Milburn, Rev. Mod. Phys. **79**, 135 (2007).
[3] P. Kok and B. W. Lovett, *Introduction to Optical Quantum Information Processing* (Cambridge University Press, 2010).
[4] T. C. Ralph, N. K. Langford, T. B. Bell, and A. G. White, Phys. Rev. A **65**, 062324 (2002).
[5] J. L. O'Brien, G. J. Pryde, A. G. White, T. C. Ralph, and D. Branning, Nature **426**, 264 (2003).
[6] M. A. Pooley, D. J. P. Ellis, R. B. Patel, A. J. Bennett, K. H. A. Chan, I. Farrer, D. A. Ritchie, and A. J. Shields, Applied Physics Letters **100**, 211103 (2012).
[7] M. Gimeno-Segovia, P. Shadbolt, D. E. Browne, and T. Rudolph, Phys. Rev. Lett. **115**, 020502 (2015), ISSN 10797114, 1410.3720.
[8] I. L. Chuang and Y. Yamamoto, Phys. Rev. A **52**, 3489 (1995), ISSN 10502947, 9505011.
[9] L. M. Duan and H. J. Kimble, Phys. Rev. Lett. **92**, 127902 (2004), ISSN 00319007, 0309187.
[10] A. Reiserer, N. Kalb, G. Rempe, and S. Ritter, Nature **508**, 237 (2014).
[11] I. Shomroni, S. Rosenblum, Y. Lovsky, O. Bechler, G. Guendelman, and B. Dayan, Science **345**, 903 (2014).
[12] T. G. Tiecke, J. D. Thompson, N. P. de Leon, L. R. Liu, V. Vuletic, and M. D. Lukin, Nature **508**, 241 (2014).
[13] H. Kim, R. Bose, T. C. Shen, G. S. Solomon, and E. Waks, Nat Photon **7**, 373 (2013).
[14] C. Wang, Y. Zhang, R.-Z. Jiao, and G.-S. Jin, Opt. Express **21**, 19252 (2013).
[15] L.-M. Duan and H. J. Kimble, Phys. Rev. Lett. **92**, 127902 (2004).
[16] J.-M. Gérard, in *Single Quantum Dots* (Springer Berlin Heidelberg, 2003), vol. 90 of *Topics in Applied Physics*, pp. 269–314.
[17] T. Volz, A. Reinhard, M. Winger, A. Badolato, K. J. Hennessy, E. L. Hu, and A. Imamoğlu, Nat Photon **6**, 605 (2012).
[18] D. Englund, A. Majumdar, M. Bajcsy, A. Faraon, P. Petroff, and J. Vučković, Phys. Rev. Lett. **108**, 093604 (2012).
[19] R. Bose, D. Sridharan, H. Kim, G. S. Solomon, and E. Waks, Phys. Rev. Lett. **108**, 227402 (2012).
[20] R. Johne and A. Fiore, Phys. Rev. A **86**, 063815 (2012).
[21] S. Xu, E. Rephaeli, and S. Fan, Phys. Rev. Lett. **111**, 223602 (2013).

[22] S. Fan, Ş. E. Kocabaş, and J.-T. Shen, Phys. Rev. A **82**, 063821 (2010).
[23] A. Nysteen, P. T. Kristensen, D. P. S. McCutcheon, P. Kaer, and J. Mørk, New J. Phys. **17**, 023030 (2015).
[24] A. Nysteen, D. P. S. McCutcheon, and J. Mørk, Physical Review A **91**, 063823 (2015), ISSN 1050-2947.
[25] A. Biberman, M. J. Shaw, E. Timurdogan, J. B. Wright, and M. R. Watts, Optics Letters **37**, 4236 (2012).
[26] H. Sekoguchi, Y. Takahashi, T. Asano, and S. Noda, Optics Express **22**, 916 (2014), ISSN 1094-4087.
[27] Y.-Z. Sun, Y.-P. Huang, and P. Kumar, Phys. Rev. Lett. **110**, 223901 (2013).
[28] E. T. Jaynes and F. W. Cummings, Proceedings of the IEEE **51**, 89 (1963).
[29] T. Ralph, I. Söllner, S. Mahmoodian, A. White, and P. Lodahl, Phys. Rev. Lett. **114**, 173603 (2015).
[30] D. Witthaut, M. D. Lukin, and A. S. Sørensen, EPL (Europhysics Letters) **97**, 50007 (2012).
[31] M. G. Thompson, A. Politi, J. C. F. Matthews, and J. L. O'Brien, Circuits, Devices Systems, IET **5**, 94 (2011).
[32] J. Wang, A. Santamato, P. Jiang, D. Bonneau, E. Engin, J. W. Silverstone, M. Lermer, J. Beetz, M. Kamp, S. Höfling, et al., Optics Communications **327**, 49 (2014).
[33] A. Martinez, F. Cuesta, and J. Marti, Photonics Technology Letters, IEEE **15**, 694 (2003).
[34] N. C. Harris, D. Bunandar, M. Pant, G. R. Steinbrecher, J. Mower, M. Prahbu, T. Baehr-Jones, M. Hochberg, and D. Englund, Nanophotonics (2016).
[35] J.-T. Shen and S. Fan, Phys. Rev. A **76**, 062709 (2007).
[36] E. Rephaeli and S. Fan, Photon. Res. **1**, 110 (2013).
[37] Note1, in Ref. [23], the interaction is reported strongest when $\sigma \sim \Gamma/v_{\mathrm{g}}$. This occurs for an emitter in a bi-directional waveguide, which effectively has twice the larger decay rate as for the single-directional problem considered in this work. Thus, when projected to this work, the strongest non-linearity is expected around $\sigma \sim 2\Gamma/v_{\mathrm{g}}$.
[38] M. A. Nielsen and I. L. Chuang, *Quantum Computation and Quantum Information* (Cambridge University Press, 2000).